Ceramics International 47 (2021) 1721–1727

Contents lists available at ScienceDirect

Ceramics International

journal homepage: www.elsevier.com/locate/ceramint

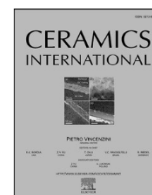

Gallium oxide films deposition by RF magnetron sputtering; a detailed analysis on the effects of deposition pressure and sputtering power and annealing

Soheil Mobtakeri [a], Yunus Akaltun [b], Ali Özer [c,d], Merhan Kılıç [e], Ebru Şenadım Tüzemen [f,g,**], Emre Gür [h,*]

[a] Department of Nanoscience and Nanoengineering, Natural and Applied Science Institute, Atatürk University, 25240, Erzurum, Turkey
[b] Department of Electrical and Electronics Engineering, Erzincan Binali Yıldırım University, 24100, Erzincan, Turkey
[c] Department of Metallurgical and Materials Engineering, Sivas Cumhuriyet University, 58140, Sivas, Turkey
[d] Advanced Technology R&D Center, Sivas Cumhuriyet University, 58140, Sivas, Turkey
[e] Department of Physics, Çukurova University, 01330, Adana, Turkey
[f] Nanophotonic Application and Research Center, Sivas Cumhuriyet University, 58140, Sivas, Turkey
[g] Department of Physics, Faculty of Science, Sivas Cumhuriyet University, 58140, Sivas, Turkey
[h] Department of Physics, Faculty of Science, Ataturk University, 25250 Erzurum, Turkey

ARTICLE INFO

Keywords:
Gallium oxide
Magnetron sputtering
Thin films
Annealing
Wide band gap semiconductors

ABSTRACT

In this study, gallium oxide (Ga_2O_3) thin films were deposited on sapphire and n-Si substrates using Ga_2O_3 target by radio frequency magnetron sputtering (RFMS) at substrate temperature of 300 °C at variable RF power and deposition pressure. The effects of deposition pressure and growth power on crystalline structure, morphology, transmittance, refractive index and band gap energy were investigated in detail. X-ray diffraction results showed that amorphous phase was observed in all the as-deposited thin films except for the thin films grown at low growth pressure. All the films showed conversion to poly-crystal β-Ga_2O_3 phase after annealing process. When the deposition pressure increased from 7.5 mTorr to 12.20 mTorr, change in the 2D growth mode to 3D columnar growth mode was observed from the SEM images. Annealing clearly showed formation of larger grains for all the thin films. Lower transmission values were observed as the growth pressure increases. Annealing caused to obtain similar transmittance values for the thin films grown at different pressures. It was found that a red shift observed in the absorption edges and the energy band gap values decrease with increasing growth pressure. For as-deposited and annealing films, increasing sputtering power resulted in the increase refractive index.

1. Introduction

The outstanding properties of metal oxide materials allow them to be used in many different application areas. Group III-oxide materials such as gallium oxide (Ga_2O_3), aluminum oxide (Al_2O_3) and indium oxide (In_2O_3) have received considerable attention recently due to their important material properties such as high chemical and thermal stability, wide bandgap and high dielectric constant. These properties make them very appropriate materials for many device applications especially for high power and solar blind photo-detector devices [1]. Particularly, Ga_2O_3 has shown industrially attractive level of high power device performances due to the large breakdown field compared to its competitive materials such as GaN, AlN, SiC and etc. [1]. Beyond high power devices, its high potentials on optoelectronic devices, on transparent conductive oxide materials, on sensors, make Ga_2O_3 important semiconductor [2] and the number of studies has increased significantly day by day.

Ga_2O_3 is a wide bandgap semiconductor, $E_g = 4.7–4.9$ eV, possessing five different phases which are commonly referred to as α, β, γ, δ and ε. Among these, α and β phases are the most stable phases and even more the β phase is thermally and chemically more stable than all other phase. Therefore, studies on gallium oxide have focused on the β phase [3–6]. Many deposition techniques have been used to produce Ga_2O_3 films such as plasma enhanced atomic layer deposition (ALD) [7], Low pressure

* Corresponding author. Department of Physics, Faculty of Science, Ataturk University, 25250, Erzurum, Turkey.
** Corresponding author. Nanophotonic Application and Research Center, Sivas Cumhuriyet University, 58140, Sivas, Turkey.
E-mail addresses: esenadim@cumhuriyet.edu.tr (E.Ş. Tüzemen), emregur@atauni.edu.tr (E. Gür).

https://doi.org/10.1016/j.ceramint.2020.08.289
Received 17 June 2020; Received in revised form 10 August 2020; Accepted 31 August 2020
Available online 2 September 2020
0272-8842/© 2020 Elsevier Ltd and Techna Group S.r.l. All rights reserved.

chemical vapor deposition (LPCVD) [8], vacuum thermal evaporation technique [9], radio frequency magnetron sputtering (RFMS) [10–14], metal organic chemical vapor deposition (MOCVD) technique [15], molecular beam epitaxy [16, 17], electron beam evaporation [18, 19], spray pyrolysis [20, 21], sol-gel [22]. Existence of these variety growth techniques is due to the easiness to obtain Ga_2O_3 compared to the nitrides and carbides.

Among these growth methods RFMS is one of the mostly used methods. This is mainly due to its easiness and being cost efficient compared to that of MOCVD, ALD, e-beam evaporation and MBE, having a faster growth rate compared to that of LPCVD, ALD, MOCVD and MBE, relatively smooth surface morphology and relatively reliable compared that of spray pyrolysis sol-gel and thermal evaporation methods. On the other hand, material grown by RFMS is amorphous phase. Therefore, most of the time heat treatment above 500 °C is generally applied, usually between 900 and 1050 °C [10, 11, 21]. This two steps growth method improves the crystal quality by reordering the randomly arranged atoms. By this method, disadvantages of the RFMS growth method is compensated.

In this study, two step growth of Ga_2O_3 were carried out by RFMS by changing growth power and growth pressure. Detailed analysis of structural, morphological and optical analysis were conducted to indicate the effects of the growth power and pressure.

2. Experimental details

Ga_2O_3 thin films were deposited by RF- magnetron sputtering via 99.99% purity Ga_2O_3 ceramic target with diameter of 2 inch and thickness of 0.125 inch that was purchased from Plasmaterials Inc. All films deposited at base pressure of approximately 5×10^{-7} Torr. Two sets of thin films were prepared and the details of growth parameters are summarized in Table 1. As given in Table 1, first set of sample were grown by changing the sputtering power, while the other parameters kept constant, such as substrate temperature at 300 °C and target to substrate distance to 7 cm. For the second set of samples, the growth pressure and thus Ar rate was changed. After Ga_2O_3 growth, possible amorphization may take place due to fast deposition rate and non-crystaline phases. Post-deposition annealing was performed in air ambient at 900 °C for 1 h to transform the crystal structures into β phase Ga_2O_3.

In order to investigate the crystalline properties, thin films were examined by θ-2θ X-ray diffraction (XRD) measurements. For XRD studies, a Rigaku Miniflex II Desktop X-ray Diffractometer system was used with Cu K_α radiation ($\lambda = 1.54059$ A) set at 30 kV and 15 mA. Diffraction was obtained in the range of $2\theta = 20$–$80°$. Scanning electron microscopy (SEM) analysis was performed using TESCAN® MIRA3 XMU at an accelerating voltage of 10 kV. Optical characterization of the samples was carried out using a double-beam UV–Vis–NIR spectrophotometer (Cary 5000). Optical transmission and absorbance spectra were taken in the wavelength range of 200–800 nm using solid sample holder accessory. Reflectance of the samples are probed by OPT-S9000 Spectroscopic Ellipsometry. The measurements were made in the wavelength range of 350–750 nm with a step size of 2 nm and at angles of incidence of 65°, 70° and 75°.

Table 1
The experimental deposition parameters of thin film coatings with changes in deposition pressure.

	Growth Pressure (mTorr)	Ar (sccm)	Temperature (°C)	RF power (Watt)
G3	7.5	15	300	100
G4	7.5	15	300	80
G6	7.5	15	300	120
G7	9.2	45	300	120
G8	10.4	75	300	120
G9	12.2	105	300	120

3. Results and discussion

3.1. Structural properties

Thin films deposited at various deposition power and pressures were analyzed with XRD measurements before and after annealing process. XRD patterns of films produced on sapphire substrate are shown in Fig. 1. Sapphire peak was observed at around 41.0° in all the thin films. As seen in the figure, no crystal peaks appeared except for the thin film G6. All the other samples showed amorphous like feature. This basically depends on the difference in the growth conditions in which the G6 sample is the one grown at highest RF power and the lowest growth pressure. Perhaps, it is due to larger energy of the Ga_2O_3 particles ejected from the target which give rise to larger adatom mobility on substrate and improves the crystal quality compared to that of other samples. In addition, lower pressure increases the growth rate which also has effect on the structural quality of grown material, G6 sample. It seems that growth pressure and the RF power does not have any influence on these as-deposited thin films. Even for this G6 sample, the intensity of the XRD peaks observed at 29.2, 36.8, and 56.8° are very small and broad. But after annealing, XRD peaks belong to Ga_2O_3 plane are appearing for all the thin films as shown in Fig. 1(b). The nature of the peak belong to the (004) is broad and shifts larger 2 theta degree especially for the G9 sample as shown in Fig. 1(b). Since there are many Ga_2O_3 XRD peaks belong to (004), (400), (002), (−202), (−401) in that 29.0–32.0° regions given in the literature [23,24], there might a few peaks close to each other to form a broad nature of the XRD peaks observed. On the other hand, the diffraction peak at 37.6° is very sharp confirming good polycrystal quality compared to that of other thin films. Two very close diffraction peaks are also observed between 55 and 60°.

The grain size of the crystals in the films was calculated from the X-ray diffraction data by using the well-known Scherrer's equation. Table 2 summarizes the XRD findings and calculated grain sizes. It is clear from the table that after annealing, peaks belong to the Ga_2O_3 appears confirming the polycrystalline nature of the grown thin films. Maximum grain size is observed for the G6 thin film as 18.7 nm. Apparently, lower growth pressure at high RF power is a good condition for the structural quality of the grown Ga_2O_3 thin films.

3.2. Surface morphology

Fig. 2 (a, b, c, g, h, i) shows SEM images for all the as-deposited Ga_2O_3 thin films grown on sapphire substrate depending on the growth power and pressure. SEM images after annealing can be seen under each SEM images of as-deposited samples as seen in Fig. 2. The growth condition of the sample G6 is a variable for both sets of the samples, i.e. for growth pressure and the power. When as-deposited samples grown at different pressures are considered, samples G6 (7.5 mTorr), G7 (9.4 mTorr), G8 (10.4 mTorr), G9 (12.2 mTorr), it is clear that there are grains formed on the surface especially as the growth pressures increases. However, after annealing, it can be seen that grain sizes get bigger. This might be indication of the crystallization of the Ga_2O_3 thin films after annealing.

There is one thing very noticeable in SEM images as mentioned above which increasing growth pressure results in columnar growth with larger feature sizes, as the growth pressure increases. This means 3 dimensional (3D) growth phase is possible at high growth pressures. On the other hand, 2D growth is seen especially for the lowest grown pressure sample G6. 2D growth mode is actually called as layer by layer or Frank-van der Merwe growth mode. In this growth mode, first whole substrate surface covered by material to be grown and then second layer grows on the first layer. On the other hand, in 3D growth mode (Volmer-Weber mode), the grown material agglomerates at some certain places and forms an island like structures on the surface. As the growth time gets longer, growth continues on those islands and the structures seen at higher pressures forms on the surface. It is possible to obtain growth

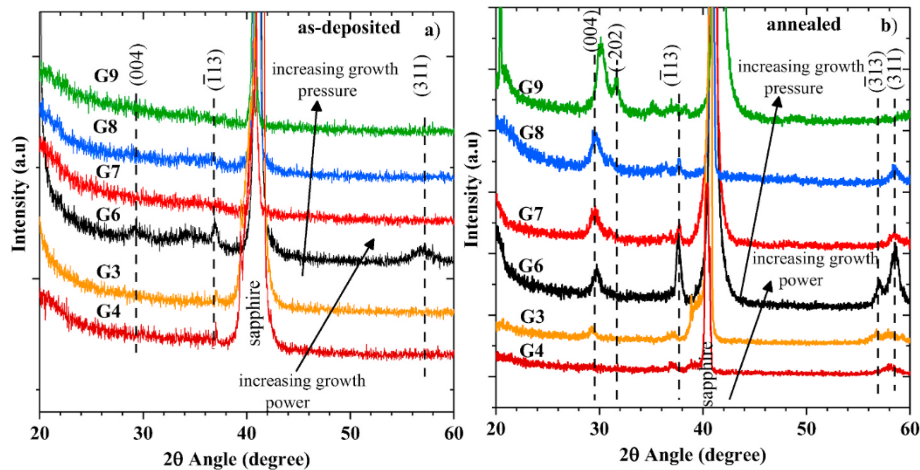

Fig. 1. XRD patterns of Ga_2O_3 thin films, as-deposited and annealed for 1 h at various deposition pressures and RF powers on sapphire substrate.

Table 2
XRD parameters of as-deposited and annealed Ga_2O_3 films at various deposition pressure and RF power on sapphire substrate.

Sample Name		2θ (deg)	FWHM (deg)	Assignments	Grain size (nm)
G3	As-deposited	amorphous			
	Annealed	37.2	0.87	(-113)	9.7
		41.1	0.23	sapphire	–
		58.0	2.64	(-313)	3.3
G4	**As-deposited**	**amorphous**			
	Annealed	29.2	–	(004)	–
		37.2	–	(-113)	–
		41.1	0.29	sapphire	–
		57.0	1.70	(-313)	5.0
G6	**As-deposited**	29.2	–	(004)	–
		36.8	–	(104)	–
		41.7	–	sapphire	–
		56.8	–	(-313)	–
	Annealed	29.5	0.75	(004)	11.2
		37.6	0.45	(-113)	18.7
		41.6	0.70	sapphire	–
		56.9	0.85	(-313)	10.1
		58.5	1.08	(311)	7.9
G7	**As-deposited**	**amorphous**			
	Annealed	29.8	0.98	(004)	8.5
		41.0	0.098	sapphire	–
		58.4	1.08	(311)	7.9
G8	**As-deposited**	**amorphous**			
	Annealed	29.8	1.20	(004)	7.0
		41.0	0.13	sapphire	–
		58.3	0.86	(311)	9.7
G9	**As-deposited**	**amorphous**			
	Annealed	30.1	0.98	(004)	8.5
		31.7	0.72	(-202)	11.6
		42.1	0.77	sapphire	–

mode changes by pressure from 2D to 3D [25]. Dislocations are formed clearly seen on the surface of the sample G6 (see larger figure size in Fig. S1). In addition, Fig. 2 (a) shows deposition at growth pressure of 9.20 mTorr and no clear grains observed similar to sample grown at 7.5 mTorr, G6. Fig. 2 (b) shows sputtered thin film at growth pressure of 10.40 mTorr and the average grain sizes are about 20–50 nm. After annealing, regular nano-sized grains were formed with almost no cracks and agglomerated particles were seen on the surface. The average particle size was measured about 40–70 nm without any agglomeration. Fig. 2(c) shows SEM image for the sample grown at pressure of 12.20 mTorr. The agglomerated particles prefer a certain orientation with the highest pressure. Annealing indicates formation of the grains on the surface of Ga_2O_3 and the grain sizes are about 100 nm.

As for the Ga_2O_3 thin films grown at same pressures of 7.5 mTorr and different RF power, namely G6, G3 and G4, Fig. 2 (g, h, i) show as-deposited sputtered sample, while lowest row **(j,k,l)** shows the annealed sputtered samples on sapphire substrates. As seen clearly, the as-deposited thin films show very smooth surface with apparent dislocations. After annealing grains are appearing on the surface and the sizes increases as the growth power decreases. There seems a difference between the lowest power grown thin films, G4, and the other two thin films. The G4 sample seems that columnar growth case is the growth mode. This growth mode might be possible, as the number of dislocations increases with decreasing growth power. This increased number of dislocations might cause the columnar growth.

3.3. Optical properties

In order to determine the optical properties of Ga_2O_3 films grown at various deposition pressures and RF power, transmittance (T %) of the films was measured wavelength range of 200–800 nm at room temperature. In order to ensure that the optical transmittance values of the films independent from the substrate absorption, transmittance measurements were done reference to the sapphire substrate. The transmittance of Ga_2O_3 thin films obtained at different pressures is given in Fig. 3 (a) and **(b)** for as-deposited and annealed samples, respectively. While the transmittance values for G6 and G7 samples are above 80% in the visible region, the transmittance decreases for sample G8 and G9 to around 70% in visible range. It is noteworthy that the transmittance of Ga_2O_3 films decreases significantly as the growth pressure increases. Color change was observed from transparent to grayish with the increasing sputtering pressure of Ga_2O_3 thin films confirming the decrease in transmittance. It might be speculated that it is due to increase in the amount of Ga in the film with increasing pressure [26]. Therefore, the transmittance values of the films decrease significantly. Annealing process supplies an extra amount of oxygen which causes the oxidation of the Ga_2O_3 thin films. As a result of this, transmittance of the thin films increase. (Please see the supplementary information Fig. S2 and **S3** for EDS measurements of the samples). As a result, the higher growth pressure give rise to non-stoichiometric growth condition. On the other hand, lower RF power condition results in the non-stoichiometric growth condition, too, as observed for G3 and G4 samples. Therefore, the samples having a lower transmittance values have non-stoichiometry in terms of Ga and O content.

The regions where the transmittance values of the Ga_2O_3 films given in Fig. 3 (a) and **(b)** are sharply decreased, as the spectra go from long wavelengths to short in the transmittance which are the band-edges of

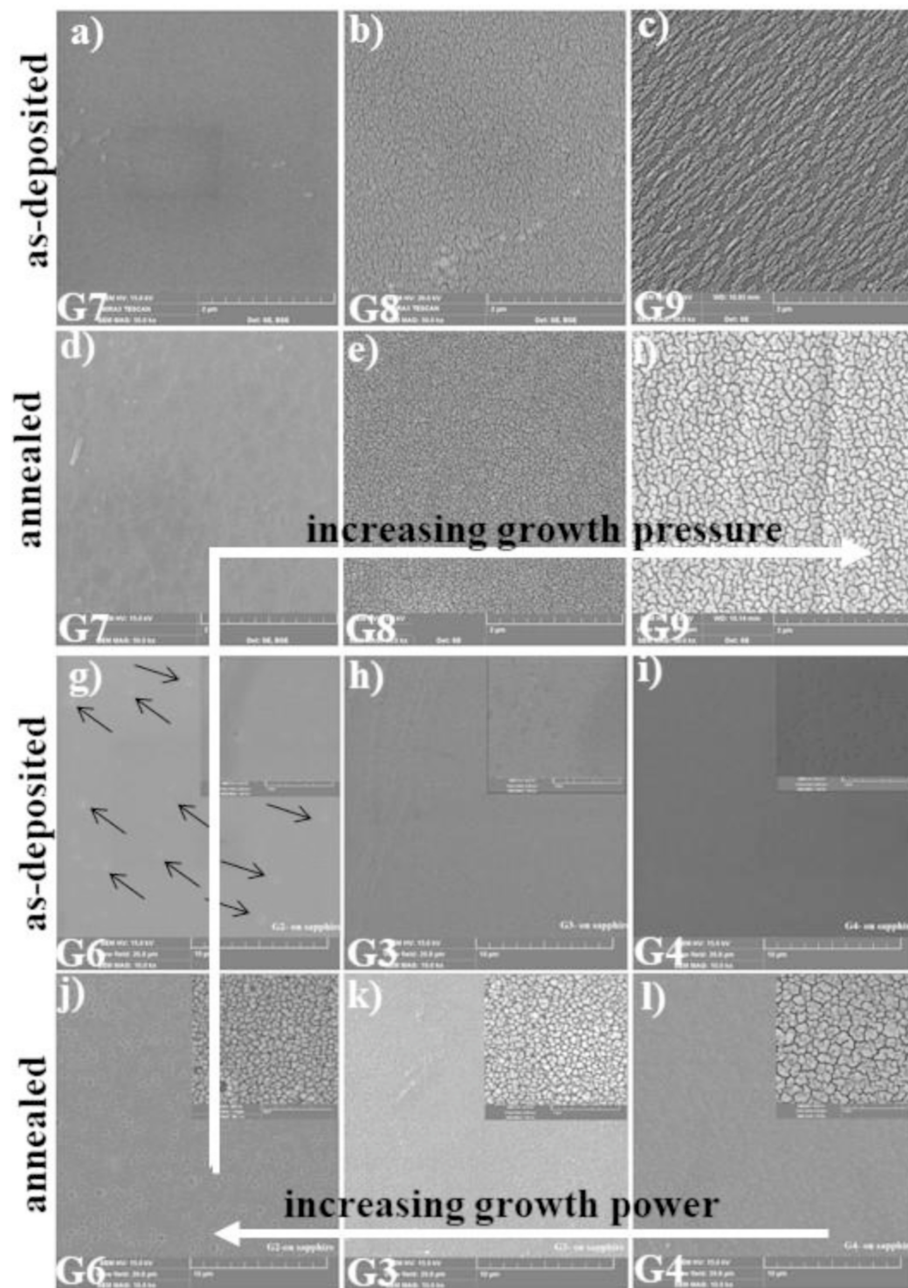

Fig. 2. SEM images of Ga_2O_3 thin films as-deposited and annealed for 1 h by RF magnetron sputtering at various sputtering pressures and power on sapphire substrate (a,b,c) as-deposited G7, G8, G9, (d,e,f) annealed G7, G8, G9 (g,h,i) as-deposited G6, G3, G4 (j,k,l) annealed G6, G3, G4.

the semiconductor Ga_2O_3. It is seen that the absorption edge of film G6 is quite sharp, but the absorption edges become flatter for the samples grown at higher pressures. This indicates the higher optical quality of the grown Ga_2O_3 thin film at the lowest pressure, namely G6. Furthermore, as shown in the transmittance spectra, as the pressure increases, the absorption edges of the films show a significant shift towards longer wavelengths as shown in Fig. 3 (a). This is an indication that increasing pressure give rise to a decrease in energy band gap values. On the other hand, the samples grown at different RF power together with G6 sample are considered, it is also seen that the absorption band-edges are very sharp similar to that of G6. This data also indicates that Ga_2O_3 thin films grown at relatively lower pressures show higher optical quality. It is also noticeable that after annealing of all the thin films show very sharp absorption band-edges and similar transmittance values except for the samples G3 and G4 grown at lower RF power.

Further investigation about the energy band gap values were made taking into consideration the absorption measurement. Absorption data are converted into the absorption coefficient by well-known Beer-Lambert laws as given below [27].

$$\alpha = \frac{1}{d} ln(T)$$

where T is the transmittance of the thin film and d is the thickness of the film. Thicknesses of the samples were measured by elipsometry measurements. The relation between the absorption coefficient and the incident photon energy and the bandgap of the material is given by [14]

$$(\alpha h\nu) = B\ (h\nu - E_g)^n$$

where B is a constant, $h\nu$ photon energy, and n is a constant equal to ½

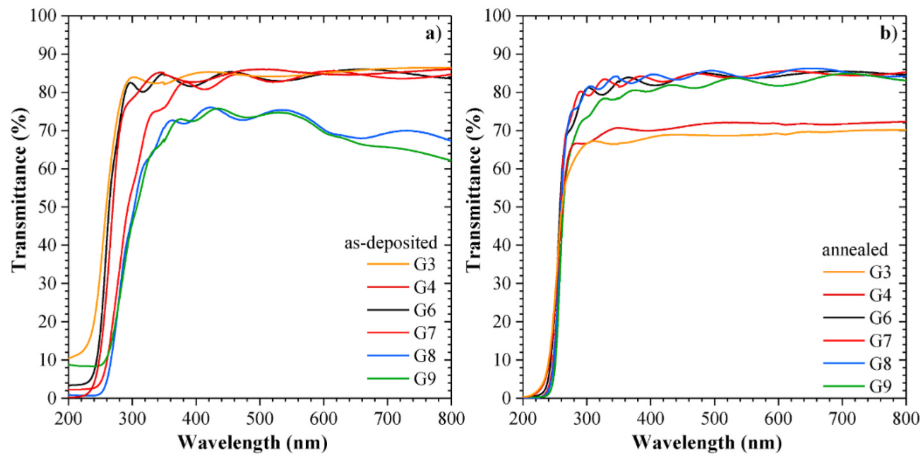

Fig. 3. Transmittance spectra of Ga_2O_3 thin films for as-deposited and annealed samples deposited at various sputtering pressures and RF power on sapphire substrate **(a)** as-deposited and **(b)** annealed films.

for semiconductors with a direct band gap transition. The energy band gap of the films was found by plotting $(\alpha h\nu)^2 - h\nu$ where the slope of this graph intersects the $h\nu$axis indicating the band gap energy of the film. Fig. 4 (a) and **(b)** show the $(\alpha h\nu)^2 - h\nu$ plots for as-deposited and annealed thin films. As seen from the figure, there is a clear shift of the band-edge absorption for the as-deposited samples. Samples grown at the lowest pressure G6 and G3 has shown the largest bandgap, as the as-deposited samples are considered. However, annealing causes the shift of absorption band-edge to higher energy for all the samples. The bandgap values and the measured thickness for the samples are tabulated in Table 3. As seen from Table 3, band gap energy values are between 4.30 and 4.90 eV, however, it changes between 4.80 and 5.00 eV after annealing.

Further detailed optical analysis was made by the spectroscopic ellipsometry technique. It provides information about the optical system that changes the polarization state of the polarized light coming onto the material. This technique is an important thin film measurement technology for its nondestructive and sensitive advantages. The change in the polarization state of the electromagnetic wave is determined by the ratio of the complex reflection coefficient and, depending on the Ψ and Δ values known as ellipsometric parameters,

$$\rho = \frac{\tilde{R}_p}{\tilde{R}_s} = \tan \Psi \ e^{i\Delta}$$

Here, ρ shows the ratio of the complex reflection coefficient, which is polarized parallel to the incidence plane $\tilde{R}_p$, and the complex reflection coefficient which is polarized perpendicular to the incidence plane $\tilde{R}_s$. [14]. The ratio of R_p to R_s, i.e. the ratio of amplitudes, gives the expression of the ellipsometric Ψ parameter.

$$\tan \Psi = \frac{R_p}{R_s}$$

The phase difference between R_p and R_s gives another ellipsometric parameter Δ.

Table 3
Bandgap energy and measured thickness values for Ga_2O_3 thin films grown at different pressures and RF powers on sapphire substrate before and after annealing.

		Thickness (nm)	Band Gap Energy (eV)
G3	As-deposited	282.3	4.83
	Annealing	266.9	4.95
G4	As-deposited	265.9	4.90
	Annealing	260.9	4.97
G6	As-deposited	424.6	4.82
	Annealing	408.8	5.00
G7	As-deposited	529.3	4.58
	Annealing	522.0	5.00
G8	As-deposited	599.0	4.57
	Annealing	543.3	4.97
G9	As-deposited	606.5	4.30
	Annealing	558.8	4.80

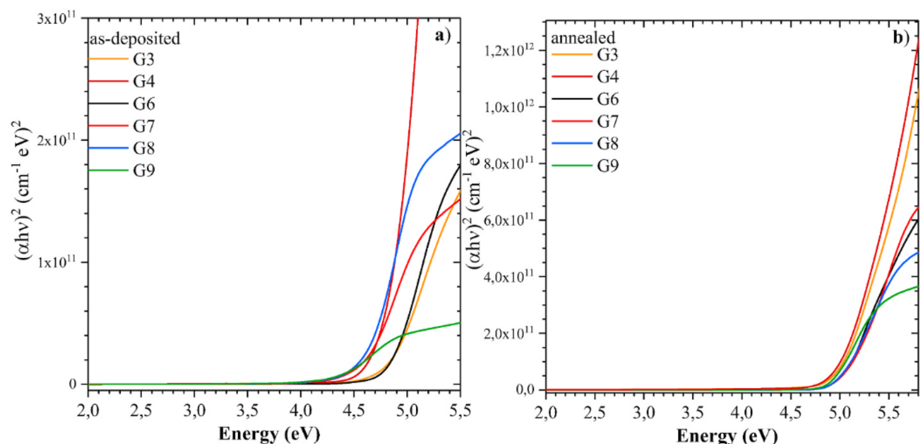

Fig. 4. At various sputtering pressures and RF powers $(\alpha h\nu)^2$ vs. hν plots for **(a)** as-deposited and **(b)** annealed films.

$\Delta = \Delta_p - \Delta_s$

Here, Δ_p and Δ_s are the phases of R_p and R_s, respectively.

The Cauchy equation is an optical model that is widely used in ellipsometric data analysis, yielding good results in the region where the material is transparent. Cauchy equation expressing the wavelength dependence of refractive index [27],

$$n = n_\infty + \frac{A}{\lambda^2} + \frac{B}{\lambda^4}$$

Here A and B are Cauchy parameters. Cauchy model should be used in areas where the extinction coefficient is zero. The model used to analyze raw ellipsometry data in this article is stacked model of $Si/SiO_2/Ga_2O_3$/Surface Roughness.

In this study, Cauchy model was selected as the model for Ga_2O_3 thin film. Therefore, considering the absorption and transmittance spectra of Ga_2O_3 films, the appropriate wavelength range for each film was determined as 350–750 nm as shown in the transmittance spectra given in Fig. 3. Since the intensity of the light on the film surface affects the intensity and phase of the light reaching the analyzer, Ψ spectra were taken by sending polarized light at different incidence angles (65°, 70° and 75°) to the surface of Ga_2O_3 films. Fitting was performed to ensure the agreement between the experimentally obtained Ψ values and theoretically determined Ψ values using the Cauchy model. Fig. 5 shows representative measurement of spectroscopic Ψ and Δ for sample G6 before and after annealing. The refractive indices of Ga_2O_3 films were determined by using the Ψ spectra where the correlation between the theoretical model and experimental data was fit the best.

The variation of refractive index of the as-deposited and annealed films grown under different sputtering pressure is shown in Fig. 6 (a) and Fig. 6 (b) on the silicon substrate. In addition, when Fig. 6 is examined, it is noteworthy that the refractive index values of Ga_2O_3 films are almost constant between the wavelength 450–750 nm for both as-deposited and the annealed samples. However, it increases a bit at lower wavelengths. It is also noticeable that increasing growth pressure results in increase in the refractive index of the Ga_2O_3 thin films. When the as-deposited and annealed thin films are compared, the values of the refractive index decreases for samples grown at higher pressures. It is believed that the change before and after annealing is due to the observed differences between the band gap energy values observed in the thin films as seen in Fig. 4. On the other hand, observed change in the transmittance might have effect on the observed difference. On the other hand, the variation is very small for the thin films grown lower pressures. This might be related similar to the observed transmittance change in the thin films after annealing. In order for clarity, samples grown at different powers were not included into the spectra given below. G3 and G4 samples show similar behavior as the G6 sample. The spectroscopic refractive index values are a bit lower, as the power decreases (Supplementary information Fig. S4).

4. Conclusions

RF-magnetron sputtering method was successfully used to grow Ga_2O_3 thin films at different growth pressures and sputtering powers on c-plane sapphire substrate. The grown thin films were annealed at 900 °C in air ambient and the effect of the annealing on the optical and structural properties of the films was investigated. All the as-deposited Ga_2O_3 thin films have shown amorphous behavior except for the sample grown at the lowest growth pressure, 7.5 mTorr. Annealing has caused to convert all the thin films from amorphous phase to polycrystal behavior. Morphological analysis has indicated that the 3D growth occurs, as the growth pressure increases. On the other hand, 2D growth with dislocations has been observed. The band gap (Eg) for

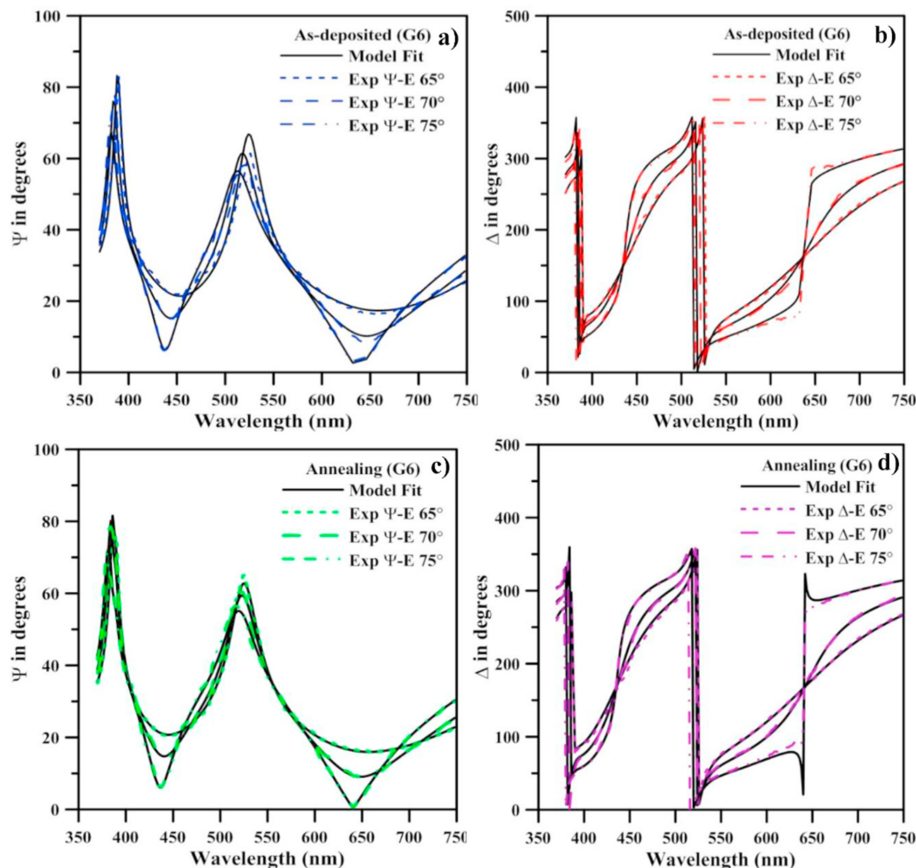

Fig. 5. The spectral dependence of Ψ and Δ for G6 film. The experimental data obtained and modeling curves are shown.

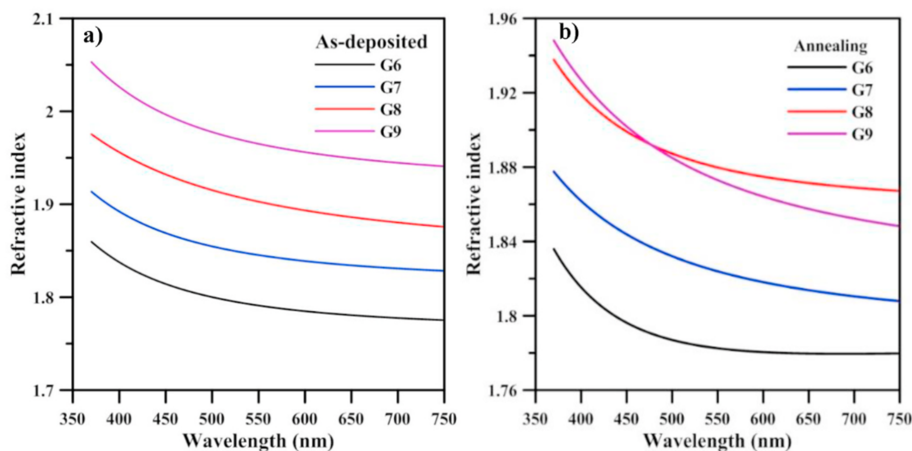

Fig. 6. At various sputtering pressures refractive index vs. wavelength plots for **(a)** as-deposited and **(b)** annealed films.

Ga_2O_3 thin films has determined from the absorption measurements. It has been found that there is a red shift in the absorption edges and the energy band gap values decrease with increasing growth pressure. The band gap of Ga_2O_3 has shown decreasing trend with increasing sputtering power. The refractive indices of Ga_2O_3 films were determined by using the Ψ spectra measured and the fit made taking into consideration of the Cauchy model. For the as-deposited and annealed films, the refractive index has increased with increasing deposition pressure. The refractive index has shown also increase with increasing sputtering power.

Declaration of competing interest

The authors declare that they have no known competing financial interests or personal relationships that could have appeared to influence the work reported in this paper.

Acknowledgments

This study was conducted in Ataturk University, Department of Physics, Faculty of Science, Sivas Cumhuriyet University R&D Center (CUTAM) in SEM Lab., Sivas Cumhuriyet University Nanophotonic Application and Research Center in Optic Lab, Cukurova University Department of Physics.

Appendix A. Supplementary data

Supplementary data related to this article can be found at https://doi.org/10.1016/j.ceramint.2020.08.289.

References

[1] S.J. Pearton, J. Yang, P.H. Cary, F. Ren, J. Kim, M.J. Tadjer, M.A. Mastro, A review of Ga_2O_3 materials, processing, and devices, Appl. Phys. Rev. 5 (2018), 011301.
[2] D. Guo, Q. Guo, Z. Chen, Z. Wu, P. Li, W. Tang, Review of Ga_2O_3-based optoelectronic devices, Mater, Today Phys 11 (2019) 100157.
[3] A. Ortiz, J.C. Alonso, E. Andrade, C. Urbiola, Structural and optical characteristics of gallium oxide thin films deposited by ultrasonic spray pyrolysis, J. Electrochem. Soc. 148 (2) (2001) F26–F29.
[4] F. Litimein, D. Rached, R. Khenata, H. Baltache, FPLAPW study of the structural, electronic and optical properties of Ga2O3: monoclinic and hexagonal phases, J. Alloys Compd. 488 (1) (2009) 148–156.
[5] D. Machon, P.F. McMillan, B. Xu, J. Dong, High pressure study of the β-to-α transition in Ga2O3, Phys. Rev. B 73 (9) (2006), 094125.
[6] M. Zinkevich, F. Aldinger, Thermodynamic assessment of the gallium-oxygen system, J. Am. Ceram. Soc. 87 (4) (2004) 683–691.
[7] David J. Comstock, Jeffrey W. Elam, Atomic layer deposition of Ga2O3 films using trimethylgallium and ozone, Chem. Mater. 24 (2012) 4011–4018.
[8] Z. Feng, Md R. Karim, H. Zhao, Low pressure chemical vapor deposition of Ga2O3 thin films: dependence on growth parameters, Apl. Mater. 7 (2019), 022514.
[9] Z. Ji, J. Du, J. Fan, W. Wang, Gallium oxide films for filter and solar-blind UV detector, Opt. Mater. 28 (2006) 415–417.
[10] M. Ogita, K. Higo, Y. Nakanishi, Y. Hatanaka, Ga2O3 thin film for oxygen sensor at high temperature, Appl. Surf. Sci. 175– 176 (2001) 721–725, 63.
[11] C. Baban, Y. Toyoda, M. Ogita, Oxygen sensing at high temperatures using Ga2O3 films, Thin Solid Films 484 (2005) 369–373.
[12] P. Schurig, M. Couturier, M. Becker, A. Polity, P.J. Klar, Optimizing the stoichiometry of Ga_2O_3 grown by RF-magnetron sputter deposition by correlating optical properties and growth parameters, Phys. Status Solidi 216 (2019) 1900385.
[13] K.H. Choi, H.C. Kang, Structural and optical evolution of Ga2O3/glass thin films deposited by radio frequency magnetron sputtering, Mater. Lett. 123 (2014) 160–164.
[14] Y. Liao, S. Jiao, S. Li, J. Wang, D. Wang, S. Gao, Q. Yu, H. Li, Effect of deposition pressure on the structural and optical properties of Ga_2O_3 films obtained by thermal post-crystallization, Cryst. Eng. 20 (2018) 133–139.
[15] D. Hu, S. Zhuang, Z.Z. Ma, X. Dong, G. Du, B. Zhang, Y. Zhang, J. Yin, Study on the optical properties of β-Ga_2O_3 films grown by MOCVD, J. Mater. Sci. Mater. Electron. 28 (2017) 10997–11001.
[16] M.-Y. Tsai, β-Ga2O3 growth by plasma-assisted molecular beam epitaxy, J. Vac. Sci. & Technol. A 28 (2010) 354.
[17] S. Ghose, S. Rahman, L. Hong, J. Salvador, R. Ramirez, H. Jin, K. Park, R. Klie, R. Droopad, Growth and characterization of β-Ga_2O_3 thin films by molecular beam epitaxy for deep-UV photodetectors, J. Appl. Phys. 122 (2017), 095302.
[18] N.C. Oldham, C.J. Hill, C.M. Garland, T.C. McGill, Deposition of Ga2O3-x ultrathin films on GaAs by e-beam evaporation, J. Vac. Sci. Technol. A: Vacuum, Surfaces, and Films 20 (3) (2002) 809–813.
[19] M.F. Al-Kuhaili, S.M.A. Durani, E.E. Khawaja, Optical properties of gallium oxide films deposited by electron-beam evaporation, Appl. Phys. Lett. 83 (22) (2003) 4533–4535.
[20] S.R. Thomas, G. Adamopoulos, Y.H. Lin, H. Faber, L. Sygellou, E. Stratakis, N. Pliatsikas, P.A. Patsalas, T.D. Anthopoulos, High electron mobility thin-film transistors based on Ga_2O_3 grown by atmospheric ultrasonic spray pyrolysis at low temperatures, Appl. Phys. Lett. 105 (2014), 092105.
[21] A. Ortiz, J.C. Alonso, E. Andrade, C. Urbiola, Structural and optical characteristics of gallium oxide thin films deposited by ultrasonic spray pyrolysis, J. Electrochem. Soc. 148 (2) (2001) F26–F29.
[22] Y. Kokubun, K. Miura, F. Endo, S. Nakagomi, Sol-gel prepared β-Ga2O3 thin films for ultraviolet photodetectors, Appl. Phys. Lett. 90 (3) (2009), 031912 – 031915.
[23] Y. An, L. Dai, Y. Wu, B. Wu, Y. Zhao, T. Liu, H. Hao, Z. Li, G. Niu, J. Zhang, Z. Quan, S. Ding, Epitaxial growth of β-Ga2O3 thin films on Ga_2O_3 and Al_2O_3 substrates by using pulsed laser deposition, J. Adv. Dielectr. 9 (4) (2019), 1950032.
[24] S. Kumar, G. Sarau, C. Tessarek, M.Y. Bashouti, A. Hähnel, S. Christiansen, R. Singh, Study of iron-catalysed growth of β-Ga2O3 nanowires and their detailed characterization using TEM, Raman and cathodoluminescence techniques, J. Phys. D Appl. Phys. 47 (2014) 435101.
[25] Y. Koçak, E. Gür, Growth control of WS_2; from 2D layer by layer to 3D vertical standing Nano-Walls, ACS Appl. Mater. Interfaces 12 (13) (2020) 15785–15792.
[26] I. Basharat, C.J. Carmalt, J.S. King, E.S. Peters, A. Tocher Derek, Molecular precursors to gallium oxide thin films, Dalton Trans. (2004) 3475–3480.
[27] C.V. Ramana, E.J. Rubio, C.D. Barraza, A.M. Gallardo, S.A. McPeak, S. Kotru, J. T. Grant, Chemical bonding, optical constants, and electrical resistivity of sputter-deposited gallium oxide thin films, J. Appl. Phys. 115 (2014), 043508.